Liver Cirrhosis Promotes Immune Escape in Hepatocellular Carcinoma via GOLM1-mediated PD-L1 Upregulation

Meng-yun Ke
firstly affiliated hospital of xi'an jiaotong university
Zhi-jin Li
Anhui Provincial Hospital
Yuan-peng Ye
the first affiliated hospital of xi'an jiaotong university
Feng-gang Ren
the first affiliated hospital of xi'an jiaotong university
Shao-ying Lu
the first affiliated hospital of xi'an jiaotong university
Xu-feng Zhang
the first affiliated hospital of xi'an jiaotong university
Rong-qian Wu
The First Affiliated Hospital of xi'an jiaotong university
Yi Lv
the first hospital of xi'an jiaotong university
Jian Dong (dongjiandoctor@126.com)
First Affiliated Hospital of Xi'an jiaotong university

Research

Keywords: Liver cirrhosis, Hepatocellular Carcinoma, Immune Escape, GOLM1

Posted Date: December 3rd, 2020

DOI: https://doi.org/10.21203/rs.3.rs-117712/v1

Abstract

Background:

Immune checkpoint blockade is considered a breakthrough in cancer treatment. However, the low response rates and therapeutic resistance of patients with hepatocellular carcinoma (HCC) represent significant challenges in the application of this treatment. Liver cirrhosis is a key driver of tumor immune escape. However, the mechanism underlying this outcome has never been clarified. This study sought to explore the role of liver cirrhosis in regulating tumor-infiltrating lymphocytes (TILs) and inducing tumor immunosuppression.

Methods:

Ninety-nine fixed HCC tissue samples were used to analyze the association between liver cirrhosis and immune escape by immunohistochemistry. H22 cells with or without GOLM1 knockdown were inoculated subcutaneously into BALB/c and BALB/c-nu/nu mice. We also created hepatocyte-specific GOLM1 transgenic mice (Alb/GOLM1 mice) and induced chemical carcinogenesis. The efficacy of anti-PD-L1 therapy combined with GOLM1 inhibition was estimated in GOLM1 -overexpressing subcutaneous model of HCC.

Results:

In HCC patients, low FIB-4 values and high $CD8^+$ T cell infiltration were correlated with prolonged survival. Elevated expression of immune checkpoints and attenuated antitumor immunity were observed in CCl4-induced mice liver fibrosis models and human fibrotic livers compared to control group. GOLM1 levels were increased in livers of patients with cirrhosis and mice in response to CCl4-induced liver fibrosis. $CD8^+$ T cell infiltrations were significantly decreased and PD-L1 expression was significantly increased in tumor tissues from Alb/GOLM1 mice compared to their corresponding control WT mice. GOLM1 induced PD-L1 expression *via* EGFR pathway activation. EGFR inhibitors, especially together with anti-PD-L1 therapy, improved the efficacy of immunotherapy in HCC.

Conclusions:

These findings illustrate the importance of liver fibrosis-induced immunosuppression as a tumor-promoting mechanism. GOLM1, which is highly upregulated in the fibrotic liver, regulates tumor microenvironmental immune escape via the EGFR/PD-L1 signaling pathway. EGFR blockade may bolster the efficacy.

Introduction

Hepatocellular carcinoma (HCC) is among the most prevalent cancer-associated causes of mortality [1, 2]. Early HCC can be treated by a variety of means, including surgical resection, radiofrequency ablation, and chemoembolization. However, there are few treatment options for advanced HCC, and the prognosis

is poor [3, 4]. Host immunity acts as a supervisor during the occurrence and development of HCC. Tumors evade adaptive immune responses through immune checkpoints. The application of immune checkpoint inhibitors (ICIs) in clinical practice has revolutionized cancer immunotherapy in the past decade[5, 6]. However, in HCC, immunotherapy has generally not produced significant clinical results due to the existence of an immunosuppressive tumor microenvironment (TME).

Liver cirrhosis is correlated with elevated HCC risk in those suffering from chronic hepatitis [7]. Furthermore, liver cirrhosis is also regarded as a vital risk factor in inducing multicentric recurrence in the remnant liver after curative resection. Liver cirrhosis presents with pathological extracellular matrix (ECM) component accumulation in the liver [8, 9]. Emerging evidence proves the important roles of tumor ECM components and highly biologically active soluble mediators (alarmins, cytokines, and chemokines) in tumor immunosuppression [10, 11], which is a major reason why fibrosis evolves into cirrhosis and HCC. Therefore, more attention should be given to the relationship between liver fibrosis and tumor immunosuppression, as immune escape that promotes the transformation of liver fibrosis into carcinogenesis or multicentric recurrence in the remnant liver after curative liver resection requires further research.

In this research, we hypothesized that Fibrosis-4 (FIB-4), which is considered a noninvasive liver fibrosis biomarker, is correlated with the immunosuppressive activity of HCC by reflecting immune checkpoint molecule expression and infiltration of $CD8^+$ tumor-infiltrating lymphocytes (TILs). We therefore conducted clinicopathological analysis of resected tumor specimens from HCC patients, and further explored the effect and the mechanism of liver fibrosis in promoting tumor immunosuppression in vivo and in vitro.

Through bioinformatic analysis, we found GOLM1 to be one of the most upregulated genes in the fibrotic liver. We confirmed that GOLM1 was highly expressed in the murine liver after carbon tetrachloride (CCl4) injection and in fibrotic liver tissue in human tissue specimens [12]. However, the relationship between GOLM1 and immune escape in the HCC microenvironment has not yet been investigated.

Herein, inhibition of GOLM1 in HCC decreased tumor growth more notably in immunocompetent mice than in nude mice by promoting antineoplastic $CD8^+$ T cell functions. In addition, the correlations among GOLM1 expression, lymphocyte numbers, and survival in human HCC were evaluated. The effects of hepatocyte-specific GOLM1 overexpression (Alb/GOLM1 mice) in a murine diethylnitrosamine (DEN)-induced HCC model that spontaneously develops autochthonous tumors were also examined. The mechanisms by which GOLM1 induces PD-L1 expression and inhibits the activity of immune cells were studied.

Materials And Methods

Clinical samples and tissue microarray

Paraffin-embedded samples of resected tumors from 99 HCC patients collected at the First Affiliated Hospital of Xi'an Jiaotong University from June 2014 - July 2018 were obtained. Clinical information was described in prior study [13]. Advanced liver fibrosis/cirrhosis was defined as FIB-4 > 3.25 [14], among the 99 patients included in tissue microarray, 54 (54.5%) were categorized as advanced liver fibrosis/cirrhosis. The medical Ethics Committee of first affiliated hospital of Xi'an Jiaotong University approved the present study, which was consistent with the 1975 Declaration of Helsinki.

Patient Data

Clinicopathologic data obtained from 186 HCC patients who underwent hepatectomy between January 2000 and December 2018 were collected at the First Affiliated Hospital of Xi'an Jiaotong University. The influence of the FIB-4 index on overall survival (OS) and disease-free survival (DFS) was evaluated.

IHC staining

Immunohistochemical (IHC) staining for PD-1, PD-L1, TIM-3, CTLA-4, IDO-1 and LAG-3 in mouse and clinical specimens was performed according to standardized institutional protocols as in prior studies [15]. Supplementary Table 3 lists primary antibodies used herein.

Cell cultures

HCC cell lines used in this study, including human HCC cell lines (Hep3B and HCCLM3) and mouse HCC cell lines (H22) were purchased from the Institute of Biochemistry and Cell Biology, Chinese Academy of Science (Shanghai China). Cells were cultured in DMEM or RPMI 1640 medium containing 10% FBS and penicillin/streptomycin at 37 ℃ with 5% CO_2.

Establishment of GOLM1 overexpressing or knocking down stable HCC cell lines

GOLM1 overexpression or shRNA knockingdown lentivirus was purchased from genechem (Shanghai, China). Cells were seeded in six-well plates for overnight and further infected with virus and polybrene. Positive clones were selected by using puromycin for following 14 days to obtain the stable cell lines.

Animal studies

Mouse GOLM1 knock-in at the H11 locus in C57BL/6N mice was performed with CRISPR/Cas-mediated genome engineering and conducted by Cyagen Biosciences Corporation (Guangzhou, China). The “Alb-mouse GOLM1 cDNA-polyA” cassette was inserted into the H11 locus (~ 0.7 kb 5' of the Eif4enif1 gene and ~ 4.5 kb 3' of the Drg1 gene). BAC clone from the C57BL/6 library as the template was used to generate homology arms by polymerase chain reaction (PCR) and the targeting vector was successfully engineered. Fertilized eggs were injected with Cas9 and gRNA with a targeting vector for mouse production. PCR and sequencing approaches were used for pup genotyping. The sequencing results are shown in Supplementary Fig. 1. Transgenic mice were bred in the medical school of Xi'an Jiaotong University. Animal care and experimental procedures were approved by the Ethics Committee of Xi'an Jiaotong University. Samples of DNA obtained from the tail were used for PCR identification of transgenic

mice. Transgene primer sequences were: F1: 5′-GCATAATAAATGTGCCCGTCG-3′, and R1: 5′-CTTTATTAGCCAGAAGTCAGATGC-3′.

The chemically induced hepatocarcinogenesis model of HCC was conducted as in prior reports [16]. Briefly, fourteen-day-old *GOLM1* transgenic (GOLM1 TG) and wild-type (WT) mice were intraperitoneally (i.p.) injected with 25 mg/kg DEN (Sigma-Aldrich, MO, USA). Fourteen days later, mice were further injected carbon tetrachloride (CCl_4, Sigma-Aldrich) dissolved in mineral oil at a dose of 0.5 mL/kg via i.p. injection once weekly for the following 20 weeks.

Induction of liver fibrosis

Eight- to ten-week-old male WT mice and their GOLM1 TG littermates were e i.p. injected twice a week with 0.5 mL/kg CCl_4 or an equal volume of mineral oil for 6 weeks and sacrificed 48 h after the last injection. The mouse serum and liver were collected for subsequent experiments.

Liver tumor model

A subcutaneous tumor model was established on 8-week-old male BALB/c mice or 4-week-old BALB/c-nu/nu mice. H22 cells were infected with GOLM1 knockdown lentivirus (H22-shGOLM1) or control lentivirus (H22-shcontrol). Then the cells (4×10^6) in PBS were collected and subcutaneously injected into the armpit of the mice. All of the mice were sacrificed following a two-week period, after which tumors were excised, weighed, paraffin-embedded, and using for IHC analyses.

Combined therapy of EGFR inhibitor gefitinib and anti-PD-L1 antibody was conducted as following. GOLM1 overexpressing H22 cells were injected subcutaneously into BALB/c mice. When these tumors were 50 mm^3, the mice were divided in to four groups: one control group was treated with an isotype control, two monotherapy groups were administered anti-PD-L1 antibody 200 μg, i.p. injection every three days) or gefitinib (6.5 mg/kg, once daily by oral gavage), one combination therapy group was treated with gefitinib and anti-PD-L1 antibody. All of the mice were sacrificed after 16 days. Then serum was isolated for detecting cytokines by using ELSIA assay. Tumors were then excised and paraffin embedded as above.

Flow cytometry

PD-L1 expressed on cell membrane was assessed via flow cytometry as in prior reports [17]. HCC cells were collected and suspended in a PBS buffer containing 0.1% BSA followed by staining for 30 minutes with PE- anti-human PD-L1 or PE- mouse IgG2b (BioLegend, CA, USA) at room temperature. Cells were then washed thrice in PBS, resuspended in PBS and further tested and assessed via flow cytometer (ACEA NovoCyte, CA, USA).

TILs were isolated from mouse tumors using a murine tumor dissociation kit (Miltenyi Biotec; Bergisch Gladbach, Germany). EDTA tubes were used to collect blood samples from mouse, and PBMC isolation via density gradient centrifugation with Pancoll (PAN-Biotec, Aidenbach, Germany) was then performed

as in prior reports [18]. TILs and PBMCs were stained with a fluorophore-labeled antibody for 30 min, washed and suspended in PBS and further analyzed by flow cytometry.

CTL cytotoxicity assay

The activity of cytotoxic T lymphocytes (CTLs) was evaluated as previously described [19]. Briefly, $CD8^+$ T cells from healthy donor blood were enriched with a RosetteSep™ Human $CD8^+$ T Cell Enrichment Cocktail (StemCell, Vancouver, BC, Canada) and further stimulated with CD3/CD28 T Cell Activator Cocktail (StemCell, Vancouver, BC, Canada) for 72 h. Then, the T cells were cocultured with target cells at the ratio indicated. The cytotoxicity of the CTLs was detected by using a cytotoxicity LDH assay kit (Dojindo, Japan).

qRT-PCR

TRIzol (Invitrogen, California, USA) was used to extract total RNAand then reverse transcribed into cDNA (Takara, Japan). Then the real-time PCR assay was conducted by using TB Green PCR Master Mix (Takara, Japan) and an ABI StepOne Plus Detection System. The results were normalized to those for GAPDH for mRNA expression measurement. The sequences of primer used were shown in supplementary table 4.

ELISA

The levels of IFN-γ, TNF-α, IL-2, IL-10 and IL-4 in the serum of the mouse were assessed using the relative elisa kit (R&D Systems, Inc, MN, USA) based on provided directions.

Immunofluorescence

Following a 15 minute fixation step using 4% paraformaldehyde, 0.5% Triton X-100 was used for permeabilization for 10 minutes, blocked using 1% BSA for 1 h, and then stained overnight with appropriate primary antibodies. Secondary anti-mouse AF488- or AF594-conjugated antibodies (proteintech, wuhan, China) were then used for staining, after which 4',6-diamidino-2-phenylindole (DAPI) (Sigma-Aldrich) was employed for nuclear staining. Finally, the slides were mounted and imaged under a Nikon A1 confocal microscope (Nikon; Minato-ku, Tokyo, Japan).

Statistical analysis

Data were compared via Student's t-tests or ANOVAs for continuous variables, whereas $\chi 2$ test or Fisher's exact tests were used to compare proportions as appropriate. Kaplan–Meier method was used to calculate survival rates and the survival differences between groups were compared using the log-rank test. The association of relevant clinicopathological variables with overall survival and disease-free survival was assessed using Cox proportional hazards models. Statistical analyses were carried out with IBM SPSS 24.0 statistical software (SPSS Inc., IL, USA). A two-sided $P < 0.05$ was the threshold of significance. For all IHC markers, the cutoff for the definition of subgroups was the median value.

Results

Liver cirrhosis is associated with poor clinical outcomes in HCC patients after liver resection

To study the prognostic role of liver fibrosis index FIB-4 in HCC patients following liver resection, we evaluated its correlation with prognosis in 186 enrolled HCC patients with liver cirrhosiss (Supplementary table 1 and table 2). The multivariate analysis showed that preoperative FIB-4 > 3.25 is an independent risk factor for OS and DFS after HCC curative resection (Fig. 1A and 1B, Supplementary table 2). To explore the relationship between liver cirrhosis and the immune microenvironment, we conducted HE staining, sirius red staining and IHC staining for α-SMA and CD8 in 99 surgically resected HCC peritumoral tissue samples (Fig. 1C). Patients with advanced fibrosis had significantly low CD8 + TIL numbers in peri-tumoral tissues than those with mild fibrosis. Further correlation analysis showed that the FIB-4 value was negatively correlated with $CD8^+$ TIL numbers (Fig. 1D). We then identified the roles of FIB-4 and $CD8^+$ TILs in predicting clinical prognosis. Survival analysis showed that higher $CD8^+$ TIL numbers tended to reflect better OS and DFS (Fig. 1E and 1F). Opposite trends were demonstrated for the FIB-4 value in OS and DFS prediction (Fig. 1G and 1H). Then, we conducted combined analysis of FIB-4 and CD8, and the data showed that patients with a low FIB-4 score and high CD8 + TIL number exhibited longer OS and DFS times than patients with other patterns (Fig. 1I and 1J). Thus liver cirrhosis may induce immunosuppression, which strongly contributes to HCC prognosis.

Hepatic fibrosis promotes immunosuppression and tumor growth

Immune checkpoint molecules are important in inducing immune suppression, but their roles in the malignant transformation process of liver fibrosis into liver cancer have not been investigated. We firstly analyzed the association between the level of liver fibrosis and the expressions of immune checkpoint molecules by analyzing the data contained in the gene chip of HBV fibrosis (GSE38941) and HCV fibrosis (GSE6764). The results shown that for HBV-fibrosis, the mRNA levels of PD-1, PD-L1, TIM-3, CTLA-4, BTLA, TIGT, IDO-1 and LAG-3 were remarkably increased compared with normal liver tissues. For HCC patients with HCV, the mRNA levels of TIM-3, CTLA-4, BTLA and IDO-1 in fibrotic tissue were significantly higher than those in normal liver tissues. In addition, there were no difference in the mRNA levels of TIM-3, CTLA-4, BTLA and IDO-1 between the fibrotic tissue and tumor tissue (Supplementary Figure 2). We then analyzed the association between the degree of liver fibrosis and the expressions of immune checkpoint molecules by performing IHC staining of α-SMA, sirius red and a series of immune checkpoint molecules (such as PD-L1, PD-1, LAG3, CTLA4, IDO-1 and TIM-3) on HCC tissue microarray (Figure 2A). The results of quantitative analysis indicated that for paracancerous tissues, the expression levels of immune checkpoint molecules in sever liver fibrosis were higher than those in mild liver fibrosis or normal liver tissue (Figure 2A and supplementary Figure 3), suggesting a positive association between the severity of liver fibrosis and immune checkpoint molecule expression in the paracancerous tissues. Meanwhile, we also found that intratumuoral immune checkpoint molecules expressions (PD-L1, LAG3, TIM-3, CTLA4 and IDO-1) were not increased compared with the adjacent tissues. Altogether, the

result indicates that the expressions of immune checkpoint molecules were elevated significantly in the process of liver fibrosis but not the HCC canceration course.

To reveal the effect of liver fibrosis on immune checkpoint molecule expression and cancer development, we successfully established a mouse liver fibrosis model by injecting CCl_4 which was confirmed by immunohistochemical staining of α-SMA and collagen Ⅰ (Supplementary figure 4). As expected, the levels of immune checkpoint molecules including PD-1, PD-L1, LAG-3, IDO-1, CTLA4 and TIM-3, were all elevated in the CCl_4-treated group compared with the control group (Figure 2B).

GOLM1 level is significantly increased in the liver fibrosis process

GOLM1 has drawn increasing attention for its high diagnostic accuracy of liver diseases including hepatitis, liver cirrhosis and liver cancer. Gene chip data (GSE89147) of CCl_4 induced liver fibrosis in mice confirmed the upregulation of GOLM1 in liver fibrosis (Supplementary figure 5A, B). IHC staining showed that the expression of GOLM1 in CCl_4-induced liver fibrosis group was significantly increased compared with the control group (Supplementary figure 5C). By analyzing the gene chip data for human liver diseases, including HBV (GSE38941), HCV(GSE38226), nonalcoholic steatohepatitis (NASH) (GSE48452) and alcoholic liver disease(GSE28619), we found that compared with the normal group, GOLM1 mRNA was significantly upregulated in these liver diseases group (Supplementary figure 5D), suggesting that the GOLM1 may play a crucial role in the pathogenesis of liver fibrosis. Further IHC staining for GOLM1 and the liver fibrosis marker α-SMA, as well as Sirius red staining in the human HCC tissue microarray demonstrated that GOLM1 expression was positively correlated with the severity liver fibrosis (Supplementary figure 5E). To assess the role of GOLM1 in liver fibrosis, CCl4 -induced liver injury model was established for WT and GOLM-TG mice. Severer inflammation and liver function injury in CCl4-injected GOLM-TG mice than in WT mice were observed. Collagen I IHC and sirius staining showed more serious liver fibrosis in CCl4-injected GOLM-TG mice than in WT mice (Supplementary Figure 6).

GOLM1 overexpression alters the immune and inflammatory profiles of the tumor site

To identify the role of GOLM1 in the tumor immune microenvironment *in vivo*, we generated transgenic mice with hepatocyte-specific GOLM1 overexpression. The high expression of GOLM1 in the mRNA and protein levels confirmed the success of transgenic mice generation (Supplementary Figure 1). We further established a classic chemically induced carcinogenesis model, the DEN/CCl_4-induced HCC model. Tumor occurrence was detected at 8 months, 10 months and 12 months. Compared with their WT counterparts, GOLM1 TG mice exhibited a higher HCC incidence, heavier liver to body weight ratio and larger tumor diameter (Figure 3A-3D). The effect of GOLM1 on the TME was evaluated further by measuring the content of immune and inflammatory cells and the expression of immune checkpoint molecules in liver tumor tissues. The flow cytometry results revealed an obvious reduction in $CD8^+$ T cell numbers and an induction of tumor-associated macrophages (TAM) ($F4/80^+CD11b^+$) in GOLM1 TG tumors compared with WT tumors (Figure 3E). There was no appreciable changes in the percentages of other immune cells, including regulatory T (Treg) cells ($CD4^+CD25^+Foxp3^+$),$CD4^+$ T cells, , B cells (CD19+)

and natural killer cells (NK1.1$^+$) (Figure 3E). Similar results were obtained in PBMCs, and GOLM1 overexpression also led to a significant reduction in CD8$^+$ T cell numbers, but other immune cell populations were not changed (Figure 3F). IHC staining of tumor tissues also observed a decrease in CD8$^+$ T cell numbers in the GOLM1 TG mouse group compared with the WT counterpart group (Figure 3G). Interestingly, we observed that the levels of α-SMA, a marker of liver fibrosis, was also elevated in the tumor tissues of GOLM1 TG mice, illustrating that GOLM1 promoted liver fibrosis *in vivo* (Figure 3G). To assess how T cell checkpoint inhibitors impact GOLM1 -induced HCC carcinogenesis, we evaluated the expression of checkpoint molecules such as PD-L1, PD-L2, TIM-3, LAG3, CTLA-4, and PD-1, in the tumor tissues of GOLM1 TG mice and WT counterparts. These analyses revealed that the mRNA expression of PD-L1 and TIM-3 was significantly increased in GOLM1 TG mice, whereas the expression levels of other immune checkpoint molecules did not change significantly (Figure 3H), the increase of PD-L1 in GOLM1 TG mice was more obvious than TIM-3. IHC staining for PD-L1 in tumor tissues also confirmed that GOLM1 overexpression induced PD-L1 expression. Together, these data indicate that GOLM1 promotes the carcinogenesis of hepatocellular carcinoma through inducing immune evasion by upregulating PD-L1 expression.

GOLM1 promotes tumor immunosuppression *in vivo*

To evaluate the role of GOLM1 in immunosuppression, we used two mice strains, including immunocompetent BALB/c mice and T cell deficient BALB/c-nu/nu mice, to establish a subcutaneous transplanted tumor model. GOLM1 knockdown inhibited tumor growth in these two types of mice (Figure 4A-4E). The tumor volume in the shGOLM1 group was 0.3 times lower than that in the control group by day 16 in BALB/c mice and 0.5-fold lower in BALB/c-nu/nu mice (Figure 4F). The result demonstrated more tumor suppression in BALB/c mice relative to the BALB/c-nu/nu mice. IHC staining of tumors from BALB/c mice presented that CD3$^+$ and CD8$^+$ T cells were infiltrated more in the GOLM1-knockdown H22 cell (H22-shGOLM1) transplanted mice than in the control cell (H22-shcontrol) transplanted mice (Figure 4G). However, α-SMA expression in the tumor site was decreased in the GOLM1 knockdown HCC cell-bearing mice, confirming the inductive role of GOLM1 in liver fibrosis (Figure 4G). Collectively, these data suggest that GOLM1 promote tumor progression by tumor immunosuppression.

GOLM1 induces PD-L1 *via* the EGFR/AKT/STAT3 pathway

To reveal the mechanism underlying GOLM1 induced PD-L1 expression, we overexpressed GOLM1 in Hep3B cells or knocked down GOLM1 expression in HCCLM3 cells by lentiviral infection. Confocal microscopy, flow cytometry and western blotting revealed that GOLM1 overexpression in Hep3B cells induced PD-L1 expression (Figure 5A-5C). In contrast, GOLM1 knockdown in HCCLM3 cells reduced PD-L1 expression (Figure 5D-5F). Further experiments of determining CTL cytotoxicity indicated that GOLM1 overexpression in Hep3B cells inhibited the cytotoxicity of CTLs (Figure 5G). In contrast, GOLM1 knocking down in HCCLM3 cells stimulated the cytotoxicity of CTLs which was impaired by anti-PD-L1 treatment (Figure 5H and 5I). Therefore, GOLM1 induced the inhibition of CTLs' activity was mediated by PD-L1.

EGFR is reportedly involved in PD-L1 regulation, and GOLM1 can also alter EGFR expression. We hypothesized that GOLM1 induces PD-L1 *via* EGFR. In order to clarify the role of EGFR in GOLM1 induced PD-L1 expression, gefitinib was used to block EGFR. Western blot analysis of the EGFR downstream signaling pathway indicated that both phosphorylation of AKT and phosphorylation of STAT3 were upregulated in GOLM1 overexpressing Hep3B cells, which was reversed by gefitinib inhibiting EGFR (Figure 5J). Flow cytometric analysis demonstrated blocking EGFR inhibited GOLM1 overexpression induced PD-L1 expression in Hep3B cells (Figure 5K). We further detected the EGFR expression in the liver tumors of GOLM1 TG and WT counterparts by IHC staining. The results presented that EGFR expression was upregulated in the GOLM1 TG mice compared with the WT mice (Figure 5L). Collectively, these results suggested that GOLM1 promoted PD-L1 expression by activating the EGFR/AKT/STAT3 pathway.

Suppression of EGFR promotes anti-PD-L1 efficacy *in vivo*

To determine whether EGFR inhibitors can enhance the HCC response to anti-PD-L1, we generated subcutaneous GOLM1-overexpressing H22 tumors (H22-GOLM1) in mice. Mice were separated into 4 groups: an isotype antibody group (control group), anti-PD-L1 alone group, GOLM1 inhibitor gefitinib alone group, and anti-PD-L1 antibody plus gefitinib group. We found that combination anti-PD-L1 and gefitinib treatment exhibited a significant tumor-inhibiting effect compared with the control and monotherapy groups without liver and kidney toxicity (Figure 6A-6C and Supplementary Figure 7). To further investigate the antitumor immune response *in vivo*, we examined the number of tumor-infiltrating T cells in the tumor sits. IHC staining results indicated that $CD3^+$ and $CD8^+$ T cell numbers were increased, and stainings of α-SMA and PD-L1 were decreased in the combination-treated group compared to monotherapy group (Figure 6D). To explore the impact of EGFR blockade on $CD8^+$T cell activity, the levels IFN-γ, TNFα and IL-2 were measured. The results presented that these cytokines were all significantly elevated in the gefitinib combined anti-PD-L1 treatment group (Figure 6E). Whereas, gefitinib or anti-PD-L1 monotherapy only slightly elevated the levels of these $CD8^+$T activated cytokines (Figure 6E). For further evaluating the effect of GOLM1 on Th1/Th2 cytokine profiles, we determined the Th2 cytokine (IL-10 and IL-4) levels. ELISAs revealed that the Th1/Th2 cytokine ratio was remarkably increased in the anti-PD-L1 and gefitinib combination treatment group compared with each monotherapy group. These results suggested the potential to enhance treatment efficacy via suppressing EGFR and PD-1/PD-L1 signaling in $GOLM1^{high}$ tumours.

Discussion

Therapies targeting PD-1 and PD-L1, well-known immune checkpoint molecules, have achieved remarkable clinical responses in multiple types of cancers, including HCC [20–22]. Unfortunately, like patients with other solid tumors, only a subset of HCC patients show durable responses, emphasizing the urgent needs to identify appropriate biomarkers for selecting patients for treatment and develop an effective strategy for nonresponders[23]. Biomarkers that can predict ICI responses include immune checkpoint ligands expression (such as PD-L1), the mutational burden, and TILs. However, these markers are still insufficient for effectively identifying patients likely to benefit from ICIs [24–28].

Liver cirrhosis, a biological program associated with qualitative and quantitative changes in ECM deposits, is considered a risk factor for chronic liver disease progression and a prognostic marker in liver cancer patients [29, 30]. Emerging evidence suggests that ECM cytoskeletal remodeling, structural plasticity and mechanical forces play crucial roles in immune cell trafficking, activation, and the formation of immunological synapses. ECM density and basement membrane makeup are controlled by stromal matrix components and determine immune cell migration and spatial distribution patterns [11, 31, 32]. We demonstrated that FIB-4, a noninvasive liver fibrosis biomarker, was significantly negatively correlated with CD8 + TILs. Since FIB-4 can reliably be assessed via routine laboratory tests, it has great clinical applicability in assess the hepatic fibrosis degree. We suggest FIB-4 as a new biomarker to select HCC patients for immune checkpoint blockade and other immunotherapies.

Additionally, the results presented here illuminate how liver cirrhosis regulates immunosuppression in the TME. Bioinformatic analysis showed that patients with a “liver cirrhosis” phenotype were associated with elevations in the levels of multiple immune checkpoint molecules. Consistent with the gene analysis results, IHC staining of human and murine tissue samples confirmed that immune checkpoint expression levels were increased mainly in cirrhotic tissue and remained constant or decreased from cirrhosis to HCC. This indicates that cirrhosis is largely to blame for the "alarming" rise in immune checkpoint expression levels, and immune escape plays a potential role in HCC initiation and progression for patient with liver cirrhosis. Liver cirrhosis might accelerate hepatocarcinogenesis not only by directly reprogramming cancer cells but also by reprogramming the immune response in the local TME.

The molecular mechanisms underlying the association between liver cirrhosis and tumor immunosuppression require further study. By using integrated gene expression analysis of liver fibrosis datasets, we demonstrated that GOLM1 expression levels were significantly increased in the fibrotic liver compared to the normal liver. GOLM1 has been reported as a useful marker for liver fibrosis grading, we herein consider GOLM1 as the major cause of immunosuppression in cirrhotic patients.

Inhibition of GOLM1 reduced tumor growth more obviously in BALB/c mice, which are immunocompetent, than in immunodeficient BALB/c-*nu/nu* mice, indicating that the deletion of GOLM1 suppressed HCC by stimulating antitumor immunity via modulation of $CD8^+$ TILs. In the DEN murine model of HCC, the numbers of $CD8^+$ T cells were decreased in GOLM1 TG tumors relative to WT tumors. Moreover, GOLM1 promoted PD-L1 expression in HCC, and analyses of clinical data from those with HCC further supported a positive relationship among GOLM1, PD-L1 and $CD8^+$ T cell infiltration. Herein, we showed GOLM1 dependent upregulation of PD-L1 as one possible mechanism whereby HCC with the “liver cirrhosis” phenotype escapes immune surveillance.

In addition, our findings highlight a new combination treatment strategy for improving immunotherapy. We showed that EGFR plays an important role in the GOLM1 dependent upregulation of PD-L1 expression. PD-L1 and EGFR inhibitors have been successful as cancer therapies. As monotherapies, these drugs seem to be insufficient to fully block cancer progression. Consistent with our findings, targeting EGFR and the PD-1/PD-L1 axis simultaneously improved treatment efficacy in HCC.

Furthermore, we determined that combined treatment reversed the immunosuppressive status of the HCC microenvironment and activated an antitumor $CD8^+$ T cell response.

In summary, the current data demonstrate a strong association between liver cirrhosis and immune evasion. In addition, we identified the GOLM1/EGFR axis as a critical regulatir of the immunosuppressive nature of the HCC microenvironment with liver cirrhosis. Targeting this pathway has the potential to remodel the immunosuppressive TIL population and improve immune checkpoint blockade efficacy in HCC.

Abbreviations

HCC, Hepatocellular Carcinoma;

CCl4, carbon tetrachloride;

PD-1, programmed cell death protein 1;

PD-L1/PD-L2, programmed cell death ligand 1/2;

CTLA4, monoclonal antibodies against cytotoxic T lymphocyteantigen 4;

TIM-3, T cell immunoglobulin and mucin domain-containing protein-3;

IDO-1, indoleamine 2,3-dioxygenase 1;

LAG-3, Lymphocyte-activation-gene-3;

BTLA, B and T lymphocyte attenuator;

TIGIT; T cell immunoreceptor with Ig and ITIM domains;

GOLM1, Golgi membrane protein;

ICIs, immune checkpoint inhibitors;

TME, tumor microenvironment;

ECM, extracellular matrix;

FIB-4, Fibrosis-4;

SMA, smooth muscle actin;

TILs, tumor-infiltrating lymphocytes;

DEN, diethylnitrosamine;

PCR, polymerase chain reaction;

SPF, specific pathogen free.

Declarations

Ethics approval and consent to participate

All procedures performed in studies involving human participants were in accordance with the ethical standards of the Research Ethics Committee of The First Affiliated Hospital of Xi'an Jiaotong University (2017-122) and with the 1964 Helsinki declaration and its later amendments. ALL written informed consent to participate in the study was obtained from HCC patients for samples to be collected from them.

All animal experiments were approved by the Animal Welfare Committee of medical school of Xi'an Jiao Tong University, and experimental methods were performed in accordance with the guidelines of medical school of Xi'an Jiao Tong University Animal Care.

Consent for publication

Not applicable.

Availability of data and material

Please contact the corresponding author (Jian Dong, dongjiandoctor@126.com) for data requests.

Competing interests

The authors declare that they have no competing interests.

Funding

This study was supported by grants from the National Natural Science Foundation

of China (81702434).

Authors' contributions

MK, and YL, RW, JD conceived and designed the experiments; MK, SL, ZL and YY performed the experiments; MK, TC and FR analyzed the data; FR, and FM contributed reagents/materials/analysis tools; MK and JD wrote the paper. All authors read and approved the final manuscript.

Acknowledgements

Not applicable.

References

[1] Bray F, Ferlay J, Soerjomataram I, Siegel RL, Torre LA and Jemal A. Global cancer statistics 2018: GLOBOCAN estimates of incidence and mortality worldwide for 36 cancers in 185 countries. CA Cancer J Clin 2018; 68: 394-424.

[2] Jemal A, Bray F, Center MM, Ferlay J, Ward E and Forman D. Global cancer statistics. CA Cancer J Clin 2011; 61: 69-90.

[3] EASL-EASD-EASO Clinical Practice Guidelines for the management of non-alcoholic fatty liver disease. J Hepatol 2016; 64: 1388-1402.

[4] Marrero JA, Kulik LM, Sirlin CB, Zhu AX, Finn RS, Abecassis MM, Roberts LR and Heimbach JK. Diagnosis, Staging, and Management of Hepatocellular Carcinoma: 2018 Practice Guidance by the American Association for the Study of Liver Diseases. Hepatology 2018; 68: 723-750.

[5] Callahan MK, Postow MA and Wolchok JD. Targeting T Cell Co-receptors for Cancer Therapy. Immunity 2016; 44: 1069-1078.

[6] Hoos A. Development of immuno-oncology drugs - from CTLA4 to PD1 to the next generations. Nat Rev Drug Discov 2016; 15: 235-247.

[7] Suh B, Park S, Shin DW, Yun JM, Yang HK, Yu SJ, Shin CI, Kim JS, Ahn E, Lee H, Park JH and Cho B. High liver fibrosis index FIB-4 is highly predictive of hepatocellular carcinoma in chronic hepatitis B carriers. Hepatology 2015; 61: 1261-1268.

[8] Magdaleno F, Arriazu E, Ruiz de Galarreta M, Chen Y, Ge X, Conde de la Rosa L and Nieto N. Cartilage oligomeric matrix protein participates in the pathogenesis of liver fibrosis. J Hepatol 2016; 65: 963-971.

[9] Friedman SL. Mechanisms of hepatic fibrogenesis. Gastroenterology 2008; 134: 1655-1669.

[10] Huse M. Mechanical forces in the immune system. Nat Rev Immunol 2017; 17: 679-690.

[11] Hynes RO. The extracellular matrix: not just pretty fibrils. Science 2009; 326: 1216-1219.

[12] Kladney RD, Cui X, Bulla GA, Brunt EM and Fimmel CJ. Expression of GP73, a resident Golgi membrane protein, in viral and nonviral liver disease. Hepatology 2002; 35: 1431-1440.

[13] Dong J, Ke MY, Wu XN, Ding HF, Zhang LN, Ma F, Liu XM, Wang B, Liu JL, Lu SY, Wu R, Pawlik TM, Lyu Y and Zhang XF. SRY is a Key Mediator of Sexual Dimorphism in Hepatic Ischemia/Reperfusion Injury. Ann Surg 2020;

[14] So-Armah KA, Lim JK, Lo Re V, Tate JP, Chang CH, Butt AA, Gibert CL, Rimland D, Marconi VC, Goetz MB, Rodriguez-Barradas MC, Budoff MJ, Tindle HA, Samet JH, Justice AC and Freiberg MS. FIB-4 stage of

liver fibrosis predicts incident heart failure among HIV-infected and uninfected patients. Hepatology 2017; 66: 1286-1295.

[15] Dong Q, Zhu X, Dai C, Zhang X, Gao X, Wei J, Sheng Y, Zheng Y, Yu J, Xie L, Qin Y, Qiao P, Zhou C, Yu X, Jia H, Ren N, Zhou H, Ye Q and Qin L. Osteopontin promotes epithelial-mesenchymal transition of hepatocellular carcinoma through regulating vimentin. Oncotarget 2016; 7: 12997-13012.

[16] Dapito DH, Mencin A, Gwak GY, Pradere JP, Jang MK, Mederacke I, Caviglia JM, Khiabanian H, Adeyemi A, Bataller R, Lefkowitch JH, Bower M, Friedman R, Sartor RB, Rabadan R and Schwabe RF. Promotion of hepatocellular carcinoma by the intestinal microbiota and TLR4. Cancer Cell 2012; 21: 504-516.

[17] Cerezo M, Guemiri R, Druillennec S, Girault I, Malka-Mahieu H, Shen S, Allard D, Martineau S, Welsch C, Agoussi S, Estrada C, Adam J, Libenciuc C, Routier E, Roy S, Désaubry L, Eggermont AM, Sonenberg N, Scoazec JY, Eychène A, Vagner S and Robert C. Translational control of tumor immune escape via the eIF4F-STAT1-PD-L1 axis in melanoma. Nat Med 2018; 24: 1877-1886.

[18] Beyer M, Abdullah Z, Chemnitz JM, Maisel D, Sander J, Lehmann C, Thabet Y, Shinde PV, Schmidleithner L, Köhne M, Trebicka J, Schierwagen R, Hofmann A, Popov A, Lang KS, Oxenius A, Buch T, Kurts C, Heikenwalder M, Fätkenheuer G, Lang PA, Hartmann P, Knolle PA and Schultze JL. Tumor-necrosis factor impairs CD4(+) T cell-mediated immunological control in chronic viral infection. Nat Immunol 2016; 17: 593-603.

[19] Barsoum IB, Koti M, Siemens DR and Graham CH. Mechanisms of hypoxia-mediated immune escape in cancer. Cancer Res 2014; 74: 7185-7190.

[20] Powles T, O'Donnell PH, Massard C, Arkenau HT, Friedlander TW, Hoimes CJ, Lee JL, Ong M, Sridhar SS, Vogelzang NJ, Fishman MN, Zhang J, Srinivas S, Parikh J, Antal J, Jin X, Gupta AK, Ben Y and Hahn NM. Efficacy and Safety of Durvalumab in Locally Advanced or Metastatic Urothelial Carcinoma: Updated Results From a Phase 1/2 Open-label Study. JAMA Oncol 2017; 3: e172411.

[21] Antonia SJ, Villegas A, Daniel D, Vicente D, Murakami S, Hui R, Yokoi T, Chiappori A, Lee KH, de Wit M, Cho BC, Bourhaba M, Quantin X, Tokito T, Mekhail T, Planchard D, Kim YC, Karapetis CS, Hiret S, Ostoros G, Kubota K, Gray JE, Paz-Ares L, de Castro Carpeno J, Wadsworth C, Melillo G, Jiang H, Huang Y, Dennis PA and Ozguroglu M. Durvalumab after Chemoradiotherapy in Stage III Non-Small-Cell Lung Cancer. N Engl J Med 2017; 377: 1919-1929.

[22] Kaufman HL, Russell J, Hamid O, Bhatia S, Terheyden P, D'Angelo SP, Shih KC, Lebbe C, Linette GP, Milella M, Brownell I, Lewis KD, Lorch JH, Chin K, Mahnke L, von Heydebreck A, Cuillerot JM and Nghiem P. Avelumab in patients with chemotherapy-refractory metastatic Merkel cell carcinoma: a multicentre, single-group, open-label, phase 2 trial. Lancet Oncol 2016; 17: 1374-1385.

[23] El-Khoueiry AB, Sangro B, Yau T, Crocenzi TS, Kudo M, Hsu C, Kim TY, Choo SP, Trojan J, Welling THR, Meyer T, Kang YK, Yeo W, Chopra A, Anderson J, Dela Cruz C, Lang L, Neely J, Tang H, Dastani HB and Melero I. Nivolumab in patients with advanced hepatocellular carcinoma (CheckMate 040): an open-label, non-comparative, phase 1/2 dose escalation and expansion trial. Lancet 2017; 389: 2492-2502.

[24] Topalian SL, Taube JM, Anders RA and Pardoll DM. Mechanism-driven biomarkers to guide immune checkpoint blockade in cancer therapy. Nat Rev Cancer 2016; 16: 275-287.

[25] Topalian SL, Hodi FS, Brahmer JR, Gettinger SN, Smith DC, McDermott DF, Powderly JD, Carvajal RD, Sosman JA, Atkins MB, Leming PD, Spigel DR, Antonia SJ, Horn L, Drake CG, Pardoll DM, Chen L, Sharfman WH, Anders RA, Taube JM, McMiller TL, Xu H, Korman AJ, Jure-Kunkel M, Agrawal S, McDonald D, Kollia GD, Gupta A, Wigginton JM and Sznol M. Safety, activity, and immune correlates of anti-PD-1 antibody in cancer. N Engl J Med 2012; 366: 2443-2454.

[26] Wolchok JD, Kluger H, Callahan MK, Postow MA, Rizvi NA, Lesokhin AM, Segal NH, Ariyan CE, Gordon RA, Reed K, Burke MM, Caldwell A, Kronenberg SA, Agunwamba BU, Zhang X, Lowy I, Inzunza HD, Feely W, Horak CE, Hong Q, Korman AJ, Wigginton JM, Gupta A and Sznol M. Nivolumab plus ipilimumab in advanced melanoma. N Engl J Med 2013; 369: 122-133.

[27] Rizvi NA, Hellmann MD, Snyder A, Kvistborg P, Makarov V, Havel JJ, Lee W, Yuan J, Wong P, Ho TS, Miller ML, Rekhtman N, Moreira AL, Ibrahim F, Bruggeman C, Gasmi B, Zappasodi R, Maeda Y, Sander C, Garon EB, Merghoub T, Wolchok JD, Schumacher TN and Chan TA. Cancer immunology. Mutational landscape determines sensitivity to PD-1 blockade in non-small cell lung cancer. Science 2015; 348: 124-128.

[28] Van Allen EM, Miao D, Schilling B, Shukla SA, Blank C, Zimmer L, Sucker A, Hillen U, Foppen MHG, Goldinger SM, Utikal J, Hassel JC, Weide B, Kaehler KC, Loquai C, Mohr P, Gutzmer R, Dummer R, Gabriel S, Wu CJ, Schadendorf D and Garraway LA. Genomic correlates of response to CTLA-4 blockade in metastatic melanoma. Science 2015; 350: 207-211.

[29] Hanahan D and Coussens LM. Accessories to the crime: functions of cells recruited to the tumor microenvironment. Cancer Cell 2012; 21: 309-322.

[30] Wang Y, Tu K, Liu D, Guo L, Chen Y, Li Q, Maiers JL, Liu Z, Shah VH, Dou C, Tschumperlin D, Voneschen L, Yang R and Kang N. p300 Acetyltransferase Is a Cytoplasm-to-Nucleus Shuttle for SMAD2/3 and TAZ Nuclear Transport in Transforming Growth Factor beta-Stimulated Hepatic Stellate Cells. Hepatology 2019; 70: 1409-1423.

[31] Hallmann R, Zhang X, Di Russo J, Li L, Song J, Hannocks MJ and Sorokin L. The regulation of immune cell trafficking by the extracellular matrix. Curr Opin Cell Biol 2015; 36: 54-61.

[32] Kato T, Noma K, Ohara T, Kashima H, Katsura Y, Sato H, Komoto S, Katsube R, Ninomiya T, Tazawa H, Shirakawa Y and Fujiwara T. Cancer-Associated Fibroblasts Affect Intratumoral CD8(+) and FoxP3(+) T

Cells Via IL6 in the Tumor Microenvironment. Clin Cancer Res 2018; 24: 4820-4833.

Figures

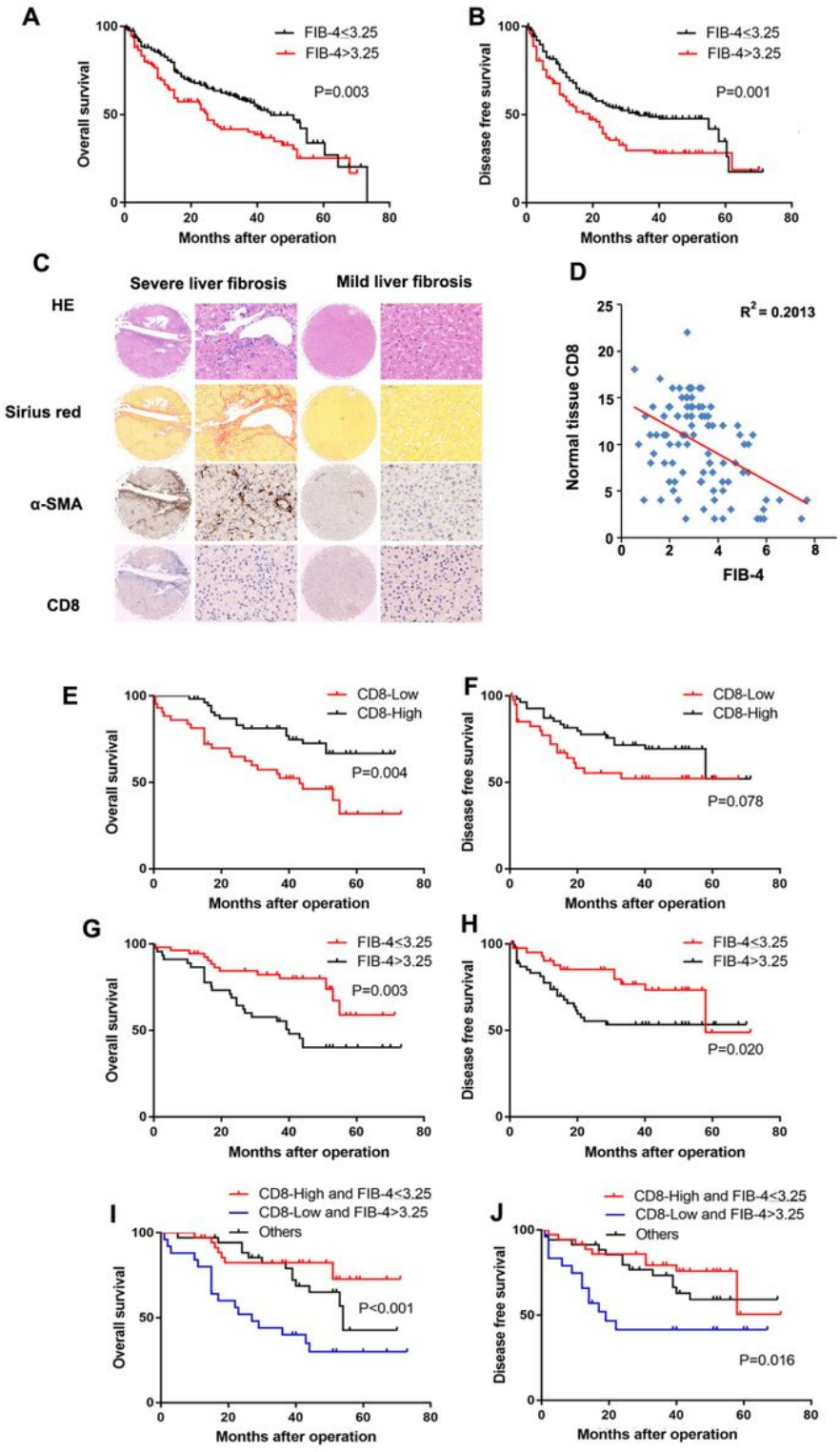

Figure 1

The FIB-4 score is correlated with CD8+ T cell infiltration in surgically resected HCC samples. A, B OS and DFS curves of patients stratified according to the FIB-4 score in peritumoral tissues are shown. The low FIB-4 score group showed a significantly worse prognosis. C, H&E and Sirius red staining and IHC staining of sections for α-SMA and CD8+ T cells; were shown. D, Correlation analysis of FIB-4 scores and numbers of CD8+ T cells in the peritumoral tissues of HCC patients was performed. E-H OS and DFS analysis were performed on CD8+T cells numbers (E, F) and FIB-4 value (G, H). I-J, Prognostic analysis combining CD8+ T cells with FIB-4 was performed.

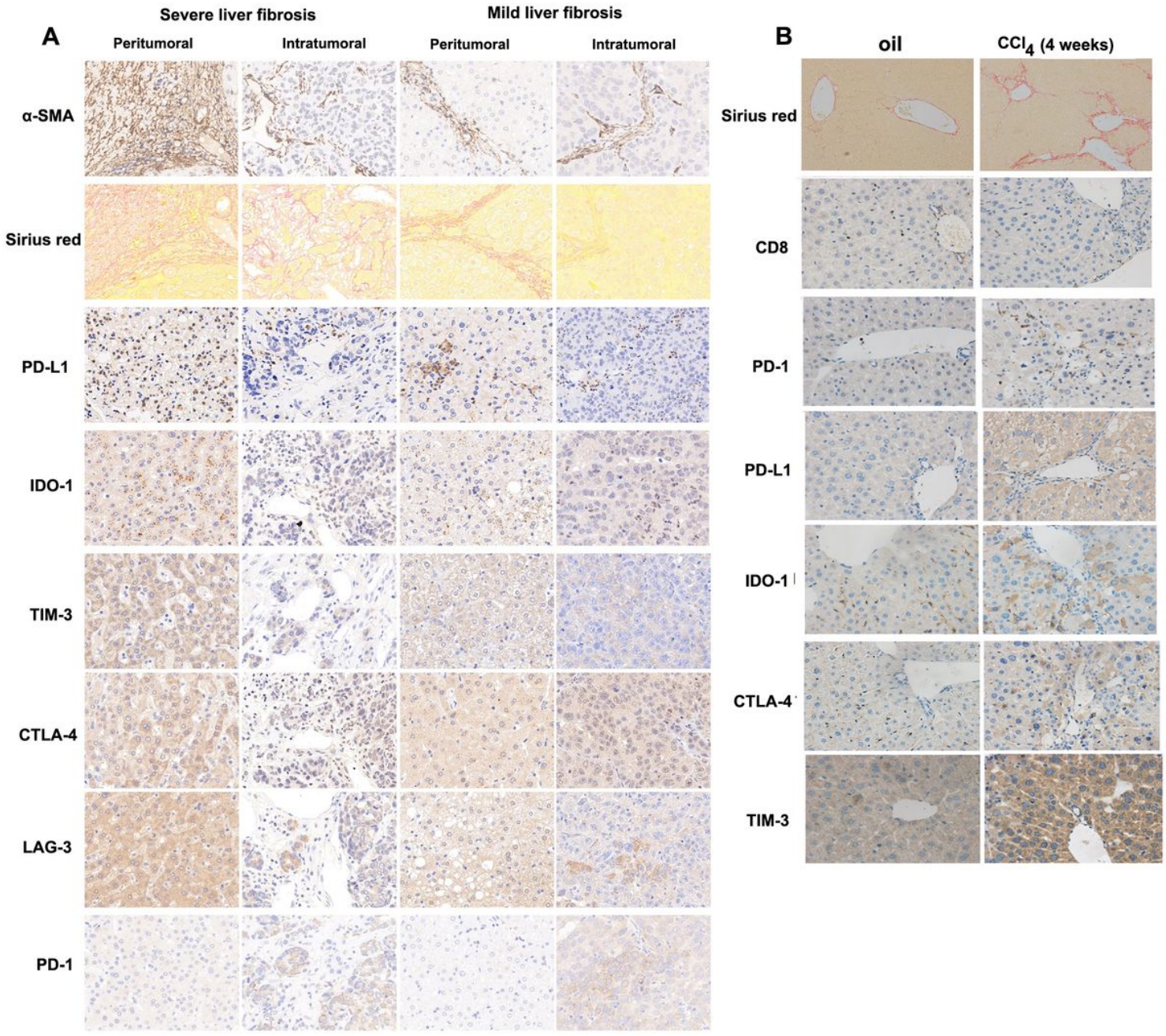

Figure 2

Liver fibrosis promotes tumor progression by inhibiting the immune system. A, IHC staining of liver fibrosis markers (α-SMA and Sirius red) and immune checkpoint molecules (PD-L1, IDO-1, TIM-3, TIM-3, CTLA-4, LAG-3, PD-1) on HCC tissue microarray were shown. B, IHC images of immune checkpoint molecules expressed in the CCl4-induced liver fibrosis mouse model were shown.

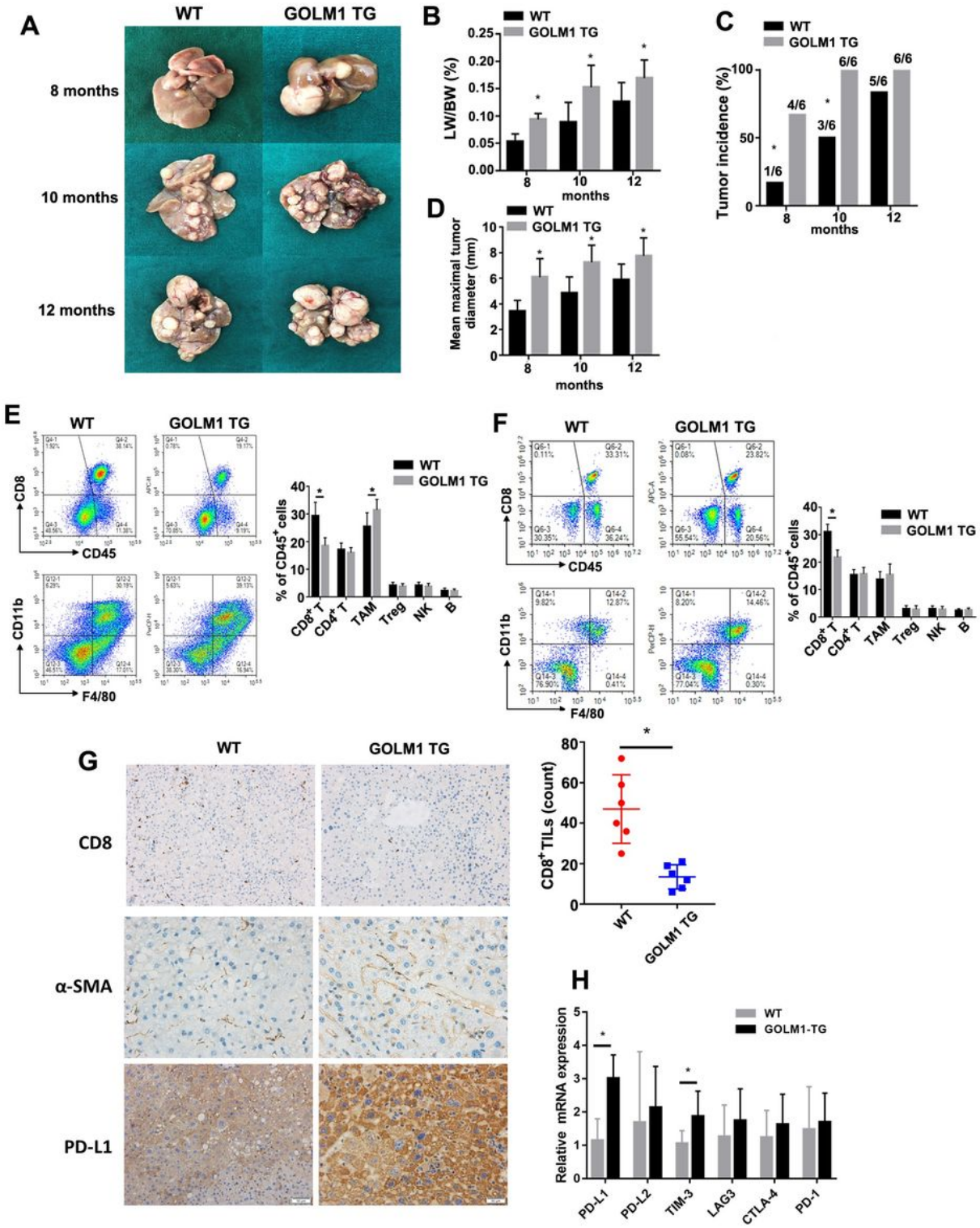

Figure 3

GOLM1 overexpression suppresses CD8+ T cell infiltration, induces HCC PD-L1 expression, and results in altered inflammatory and immune profiels in mice experiencing DEN/CCl4-induced hepatocarcinogenesis in male WT mice (n=6) and male GOLM1 TG mice (n=6). A, Representative images of the mouse livers at 8, 10, and 12 months were shown. B-D, Size of tumor in livers were evaluated by calculating the liver weights to body weights ratio (B), counting the incidence of tumor (C) and measuring the diameter of the tumor (D). E-F, Immune cells, including CD4+T cells, CD8+ T cells, Tregs, NK cells, B lymphocytes and TAMs in liver tumor tissues (E) and PBMCs (F) were detected by flow cytometry. Left: representative flow plots indicating the proportions of CD8+ T cells and TAMs. Right: comprehensive results of the percentage of immune cells. G, Representative images of CD8, α-SMA and PD-L1 immunostaining of liver tumor tissue sections from WT and GOLM1 TG mice were shown. H, The mRNA levels of indicated immune checkpoint molecular genes were determined by qPCR assay. N=6/group, Data are means ± SD; *P<0.05, for GOLM1 TG mice vs WT mice.

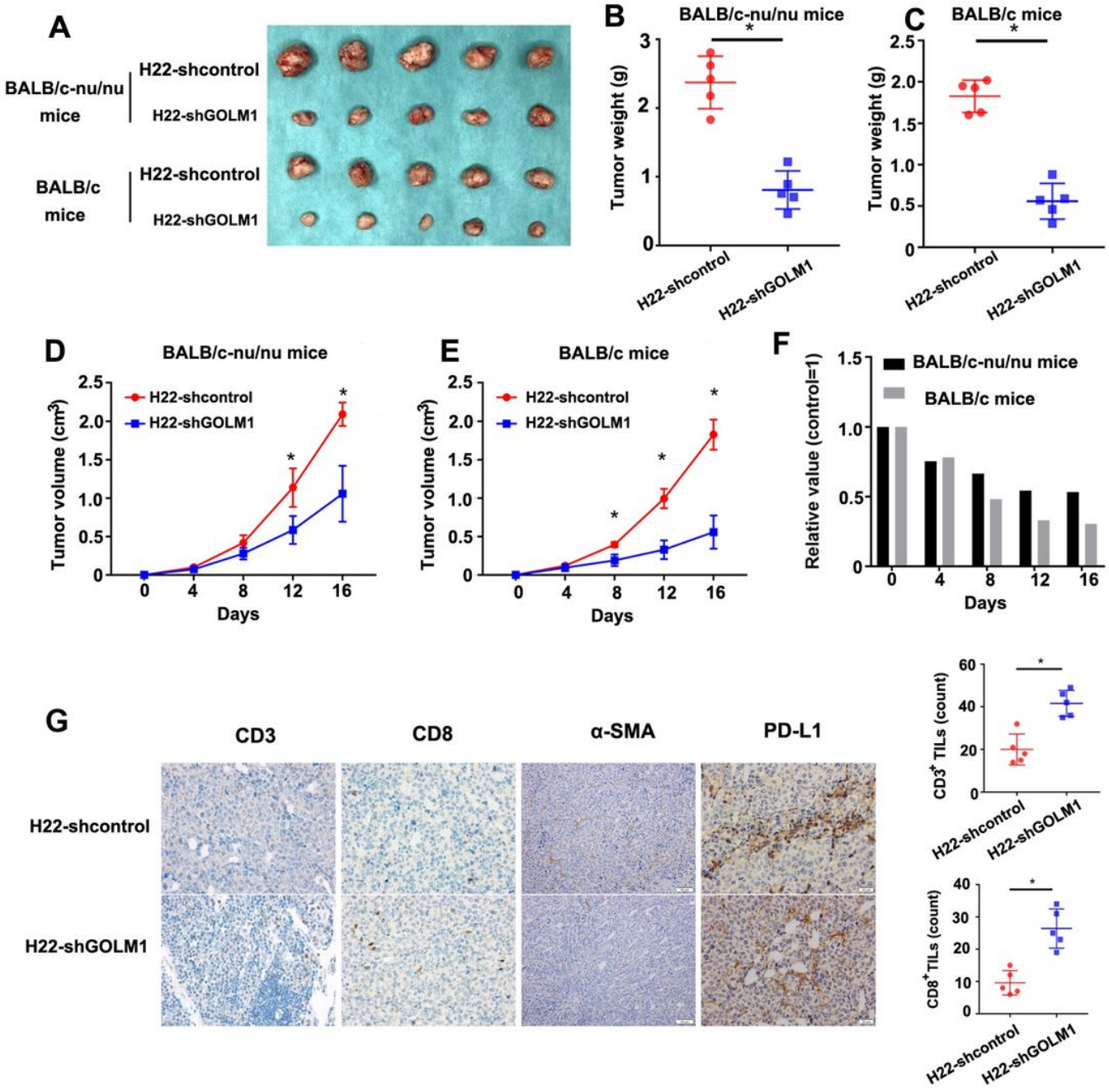

Figure 4

GOLM1 promotes tumor growth by regulating TILs in vivo. Subcutaneous tumors formed with H22-shcontrol cells or GOLM1 koncking down H22-shGOLM1 cells in BALB/c-nu/nu mice and BALB/c mice. A, Image of tumors in each experimental group was shown. B-C, Tumor weights were analyzed. D-E, Tumor volumes of each mouse were quantified every second day and the tumor growth curves were drew. F, Relative progression of tumor growth was calculated in the BALB/c-nu/nu mice and BALB/c mice. G, IHC staining for CD3, CD8, α-SMA, and PD-L1 in tumor tissues from BALB/c mice (n=5/group). Data are means ± SD; *P<0.05 vs. control.

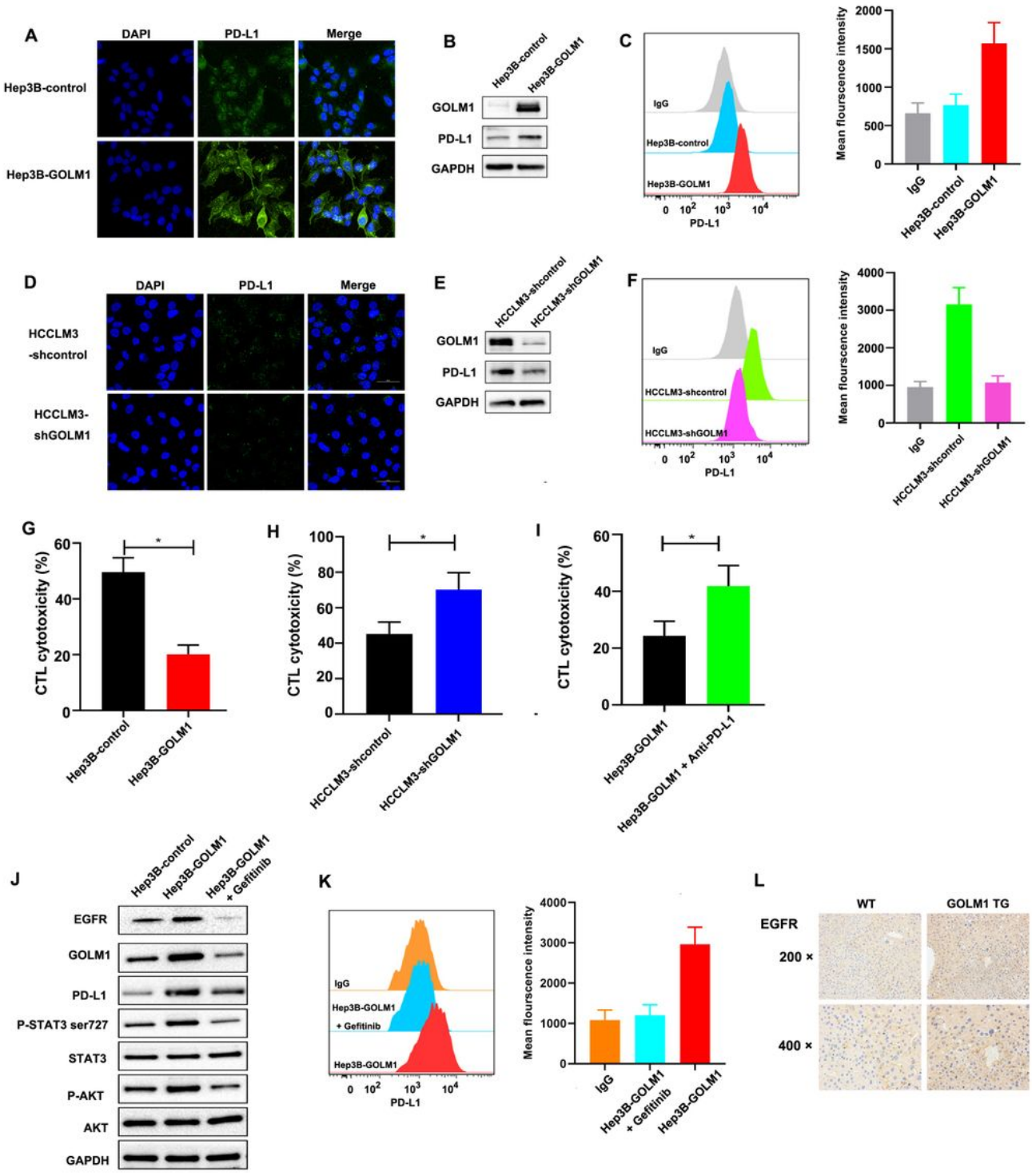

Figure 5

EGFR blockade reverses the GOLM1 -induced PD-L1 upregulation in HCC. A-F, GOLM1 overexpression in Huh7 cells facilitates PD-L1 expression (A-C), and GOLM1 knockdown in HCCLM3 cells prevents PD-L1 expression (D-F). (A, D) Confocal images, (B, E) western blot results and (C, F) flow cytometry results are shown. G-I, The GOLM1 -induced inhibition of CTL activity was mediated by PD-L1. G, GOLM1 overexpression in Hep3B cells inhibited CTL cytotoxicity. H, Knocking down GOLM1 expression in

HCCLM3 cells enhanced CTL cytotoxicity. I, Pretreatment of GOLM1 -overexpressing Hep3B cells with an anti-PD-L1 antibody reversed CTL activity. J-K, Hep3B-GOLM1 cells were treated with gefitinib (10μM) or isotype IgG for 48 h, then the cells were harvest for flow cytometric analysis and western blotting. The results showed that blocking EGFR in HCC cells inhibited GOLM1-mediated activation of the MAPK/STAT3/PD-L1 signaling pathway. L, IHC staining for EGFR in CCl4/DEN-induced HCC tissue sections showed that EGFR levels were increased in GOLM1 TG mice.

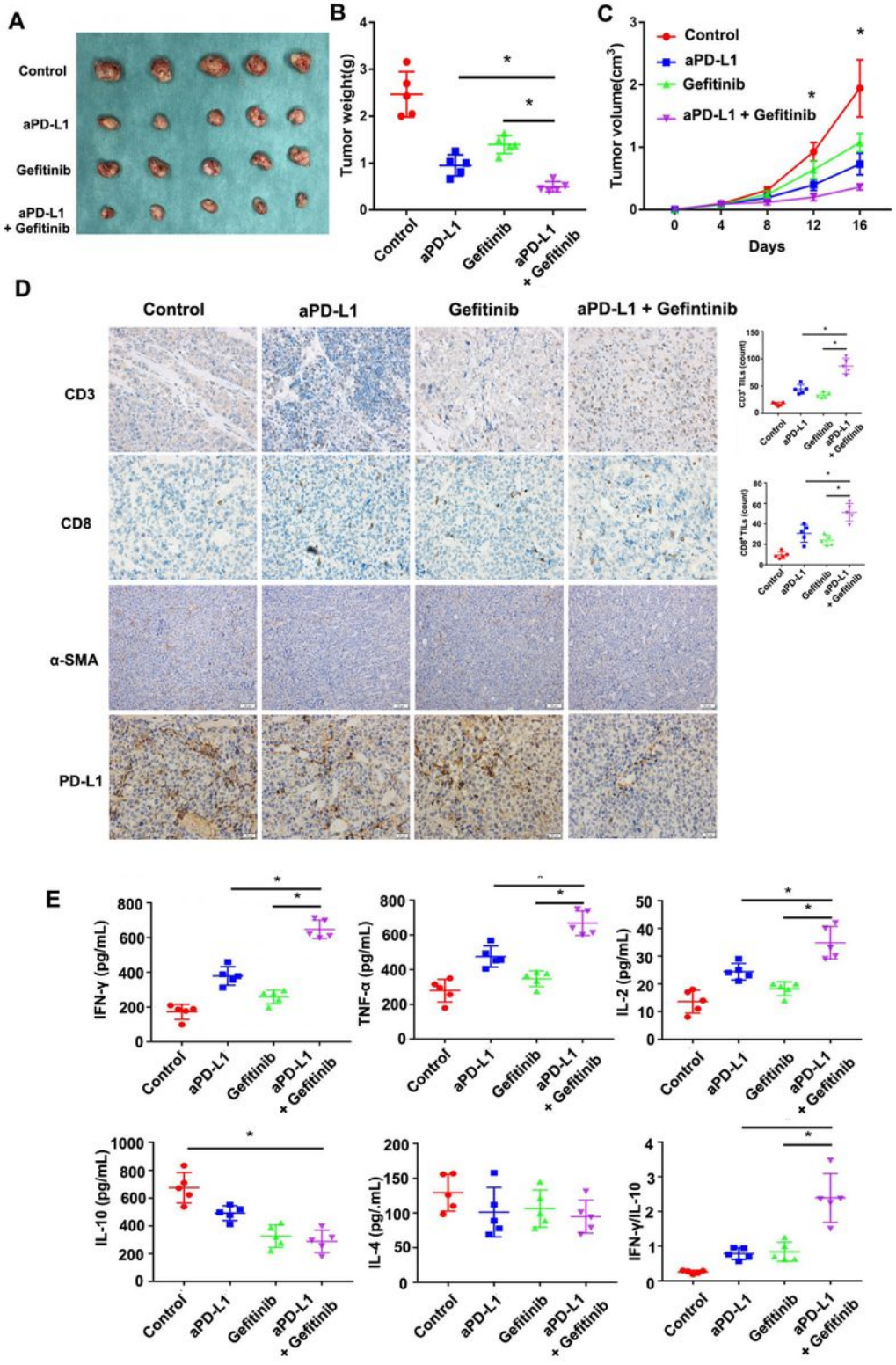

Figure 6

Combination therapy with an EGFR inhibitor and anti-PD-L1 antibody increases intratumoral T cell activation. A, Representative image of the tumors from each group was shown. B-C, The tumor weight of each group (B) and the tumor growth curves (C) were indicated. D, IHC stainings of CD3, CD8, α-SMA and PD-L1 were conducted. IHC images of CD3 and CD8 staining (left) and relative quantitative analysis (right) indicated that the infiltrations of CD3+ and CD8+ cells was significantly increased in the anti-PD-L1 antibody and gefitinib combination treatment group. F, The cytokines representing T cell activation, including Th1 cytokines (IFN-γ, TNF-α, IL-2) and Th2 cytokines (IL-4 and IL-10), in each group were analyzed by ELISA.

Supplementary Files

This is a list of supplementary files associated with this preprint. Click to download.

- Supplementarymaterials1tables.docx
- supplementarymaterials2figures.docx